

## Timely Mapping of Crop Stage and Watering Events Through Sentinel-L Time-Series

Iannini, Lorenzo; Molijn, Ramses; Alfieri, Silvia; Steele-Dunne, Susan; Menenti, Massimo

**DOI**

[10.1109/IGARSS.2018.8518906](https://doi.org/10.1109/IGARSS.2018.8518906)

**Publication date**

2018

**Document Version**

Final published version

**Published in**

IGARSS 2018 - 2018 IEEE International Geoscience and Remote Sensing Symposium

**Citation (APA)**

Iannini, L., Molijn, R., Alfieri, S., Steele-Dunne, S., & Menenti, M. (2018). Timely Mapping of Crop Stage and Watering Events Through Sentinel-L Time-Series. In J. Moreno (Ed.), *IGARSS 2018 - 2018 IEEE International Geoscience and Remote Sensing Symposium* (Vol. 2018, pp. 196-199). IEEE.  
<https://doi.org/10.1109/IGARSS.2018.8518906>

**Important note**

To cite this publication, please use the final published version (if applicable).  
Please check the document version above.

**Copyright**

Other than for strictly personal use, it is not permitted to download, forward or distribute the text or part of it, without the consent of the author(s) and/or copyright holder(s), unless the work is under an open content license such as Creative Commons.

**Takedown policy**

Please contact us and provide details if you believe this document breaches copyrights.  
We will remove access to the work immediately and investigate your claim.

# TIMELY MAPPING OF CROP STAGE AND WATERING EVENTS THROUGH SENTINEL-1 TIME-SERIES

*Lorenzo Iannini, Ramses Molijn, Silvia Alfieri, Susan Steele-Dunne, Massimo Menenti*

Delft University of Technology

## ABSTRACT

Reliable and timely mapping of crop growth conditions and of their water resources is considered a priority application in light of the abrupt climate changes. With this view, the paper presents a novel approach that makes use of dense C-Band time-series for the timely estimation of crop growth stages and for the detection of changes in crop water conditions, especially related to precipitation and irrigation events. Aided by vegetation indexes extracted from Landsat and Sentinel-2 imagery, the proposed Sentinel-1 centered method exploits both temporal patterns of crop growth and spatial patterns of water anomalies to enhance its classification robustness.

**Index Terms**— Synthetic Aperture Radar, C-Band, Sentinel, data assimilation, land cover mapping, soil, agriculture, precipitation, irrigation.

## 1. INTRODUCTION

A robust and timely mapping of land cover in terms of biomass characteristics and water availability represents a key factor for modelling land and atmospheric processes at mesoscale levels as well as for triggering actions in vegetation management at district or smaller scale levels. The latter case includes all the crop management and irrigation practices aimed at achieving an optimal trade-off between productivity and water usage. It is foreseen that the systematic use of high resolution satellite data for the estimation of crop growth stage, crop health and soil moisture would significantly augment the performances of water and energy balance models in addressing the crop needs.

In such context, active microwave sensors are deemed to play a crucial role due to their all-weather nature. Especially in the short term, C-Band imagery is expected to rapidly increase its popularity due to the global availability and the short revisit of the Sentinel-1 observations. However, interpreting backscatter dynamics and hence disentangling the geometric and dielectric variables in the radar signal is a challenging task. Several model formulations have been proposed through the last decades for both bare and vegetated soil [1]. The most explanatory ones range from semi-empirical models such as the popular Oh model for bare soil [2] and the Water Cloud Model [3] for vegetated land to radiative trans-

fer models where more complex electromagnetic interaction elements are addressed. The use of the former is in general favoured due to their simplicity and larger adaptability. A basic backscattering principle accounted by all the models is its sensitivity to the media water content, as a result of high permittivity of water ( $\epsilon_r = 80$ ) contrasting with the low one of dry matter ( $\epsilon_r = 3$ ). The sensed water belongs to the top layer of the land medium, where the layer height, or depth, depends on the penetration capability of the waves. Whereas L-band receives major signal contributes from the soil even with high crop canopies and hence can sense soil moisture directly, C-band at common incidence angles ( $30^\circ$ - $40^\circ$ ) mainly responds to the water content in vegetation when this latter has  $LAI > 2 m^2/m^2$  [4]. It is indeed acknowledged [5] that the extent of moisture changes and precipitation events on radar data heavily depend on the canopy thickness.

Despite the intrinsic sensitivity issues, several research initiatives have been recently conducted on the use of C-band for the inference of water-related quantities, most notably in two different directions: 1) the downscaling of soil moisture products [6, 7, 8], especially after the failure of the L-band active SMAP instrument, 2) the indirect estimation of precipitation through its soil moisture proxy [9, 10]. Most of this research is aimed at regional or global scale, with grid resolutions larger than 100 m and coarse assumptions on the vegetation and soil patterns. This might not be sufficient for agricultural contexts, which are temporally dynamic and spatially heterogeneous, with the human intervention (e.g. irrigation) that adds to the climatic behavior. The present paper is aimed at laying the foundations for the use of C-band SAR in near-real time crop stage estimation and watering events detection. With watering events we refer to both precipitation and irrigation as well as their discrimination based on the difference in their spatial patterns. The retrieval method is based on a two-step algorithm that estimates in turn the crop stage and conditions per field by a Hidden Markov Model methodology [11] and evaluates the likelihood of water change conditions on a larger spatial scale. The concept of this study has been developed on a large pilot test area, the Sao Paulo state (Brazil). An analysis per vegetation density and rain scenario of the radar backscatter has been here conducted and used as empirical basis for devising the approach. The method will be also applied to the Abda-Doukkala (Morocco) demonstration

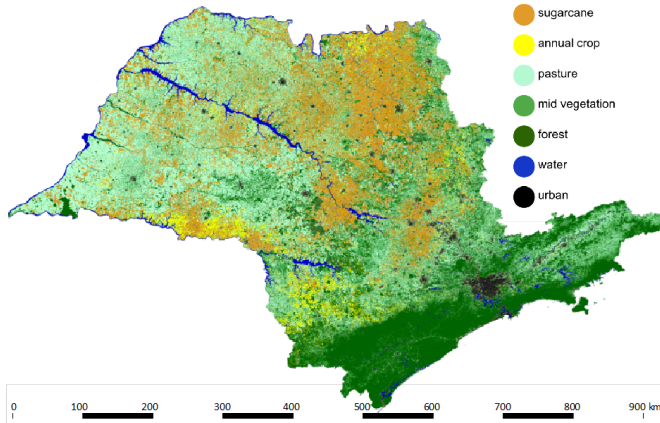


**Fig. 1.** Land cover map of the Sao Paulo state (Brazil) for year 2010.

area with a controlled irrigation system, in order to test its integrability into the crop water demand system implemented for the H2020 project MOSES (Managing crOp water Saving with Enterprise Services).

## 2. STUDY AREA AND DATA

The study is conducted on two different types of experiment sites:

- the Sao Paulo state (Brazil). This area was conveniently used for pilot conception and experimentation due to the extensive land cover mapping activities conducted for previous research projects. The application of the Hidden Markov Model approach to the Landsat NDVI and NDWI series [11] led to the generation of semi-monthly land cover maps, see Fig. 1. The vegetation mainly consist in rain fed crops and pastureland. Two years, from 2015 to 2016, were examined.
- the Abda-Doukkala test site, shown in Fig. 2. The site has been surveyed during 2016 and 2017 growth season to collect crop type and condition information. Irrigation data, aggregated per district, are also released by Office Regional de Mise en Valeur Agricole des Doukkala (ORMVAD), the local agriculture authority.

For all the study areas Sentinel-1 IW products are used in combination with the surface reflectances from the cloud-free Landsat-8 and Sentinel-2 (this latter only for the MOSES test sites) imagery. Both weather stations and Global Precipitation Measurement (GPM) satellite data are used to train and validate the technique.

## 3. METHOD AND DISCUSSION

The conceived approach is based on a temporal and spatial statistical description of the different land cover states identi-



**Fig. 2.** Demonstration area (highlighted by a red rectangle) in the Abda-Doukkala region (Morocco).

fied in each area. With the terminology 'states' we can refer to the smallest (non-aggregated) elements in the chosen taxonomy, that might refer to a specific land cover type in a specific condition, e.g. wet maize in mature stage. The satellite observations generated by the  $i$ -th state,  $S_i$ , at time  $t$  are here-with modelled through the multivariate gaussian distribution  $\mathbf{y}(t) \sim \mathcal{N}(\mathbf{m}_i(t), \mathbf{C}_i(t))$  with

$$\mathbf{m}_i(t) = [ NDVI_i(t) \quad HV_i(t) \quad \Delta HV_i(t) ]^T$$

$$\mathbf{C}_i(t) = \begin{bmatrix} v_{NDVI,i}(t) & 0 & 0 \\ 0 & v_{HV,i}(t) & \chi_i(t) \\ 0 & \chi_i(t) & v_{\Delta HV,i}(t) \end{bmatrix}$$

where  $NDVI$  stands for the expected Normalized Difference Vegetation Index,  $HV(t)$  is the expected cross-polarized backscatter in dB at time  $t$  and  $\Delta HV_i(t) = HV_i(t) - HV_i(t-1)$ , i.e. the expected difference between two consecutive acquisitions from the same Sentinel-1 beam mode and hence separated by either 6 or 12 days. Notice that the SAR and optical acquisitions are assumed independent and that the distribution becomes bivariate if optical imagery (LS8 or S2) is not available. The dependency on time  $t$  can be simplified into a dependency on the day of year for some classes or, in the case of crop states, it can be omitted, as elucidated in [11].

In order to map watering events, each model state is further exploded in four different sub-states, each related to a different scenario. The following water(ing) scenarios are addressed

DD	Dry to Dry
WW	Wet to Wet
DW	Dry to Wet
WD	Wet to Dry

They based on pairs  $(t,t-1)$  of images and are intuitively aimed at exploiting the backscatter sensitivity to water

changes. The state  $S_i$  can be now described by the index pair  $S_i \rightarrow S_m^\omega$  with  $m$  standing for the land cover type and  $\omega = \{DD, WW, DW, WD\}$  for the water scenario. The state sequence  $Q = q_1 q_2 \dots q_T$  for each pixel is modelled in time by a Markov chain, i.e. by linking probabilistically the state at time  $t - 1$  with the state at time  $t$  through the transition coefficients  $a_{m_1, \omega_1}^{m_2, \omega_2} = P(q_t = S_{m_2}^{\omega_2} | q_{t-1} = S_{m_1}^{\omega_1})$  satisfying  $\sum_{m_2} \sum_{\omega_2} a_{m_1, \omega_1}^{m_2, \omega_2} = 1$ . Model adherence to reality shall be enabled by forcing for each land cover type  $m$  the the transitions  $WW \rightarrow DD, DD \rightarrow WW, WD \rightarrow WD, DW \rightarrow DW, WD \rightarrow WW, DW \rightarrow DD$  to have a null coefficient  $a$ .

The approach implementation comprises a training/analysis phase and an inversion/verification phase. The calibration phase is aimed at estimating the model  $\lambda = (a, \mathbf{m}, \mathbf{C})$ , which results in a challenging task if rigidly approached. For the sake of simplicity, the transitions and the signature parameters  $\mathbf{m}$  and  $\mathbf{C}$  have been first estimated for each crop without discriminating between different water scenarios. The estimation is carried out by Likelihood Maximization through a Simulated Annealing technique and is applied only to  $NDVI$  and  $HV$  sequences. The results for the Sao Paulo state show the information brought by the two indicators is complementary with only partial correlation, see Fig. 3. In a second step, each state of the crop and vegetation classes (the points in Fig. 3) have been then associated to one of the 4 generic vegetation profiles based on expert knowledge: 1. bare soil or marginal vegetation, 2. low vegetation, 3. medium vegetation, 4. dense/high vegetation. These generic profiles have been could be characterized basing on the a-priori information provided by available the land cover maps and growth timing, on the available weather station data, and on the GPM precipitation estimates. The  $HV - \Delta HV$  profiles could be hence retrieved. The results are in line to our expectations, see Fig. 4 and 5, as the dependence on the vegetation density of the rain events on the backscatter is very evident.

The inversion phase, i.e. the application of the approach for retrieving the land cover information, relies on two fundamental steps:

1. Given some initial land cover state probability, the hidden Markov model  $\lambda = (a, \mathbf{m}, \mathbf{C})$  can be applied to the data sequences  $\mathbf{y}_1 \dots \mathbf{y}_T$  at each new acquisition  $T$  through the so-called forward-backward algorithm. Such solution conveniently allows to compute the log-probabilities

$$l_k(m, \omega, t) = P_k(q_t = S_m^\omega | \mathbf{y}_1 \dots \mathbf{y}_T)$$

for every spatial cell  $k$ . Notice that such probabilities are computed per cell individually.

2. The probabilities  $p_k$  are spatially aggregated per water scenario, according to

$$L(\omega, t) = \sum_k \sum_m l_k(m, \omega, t)$$

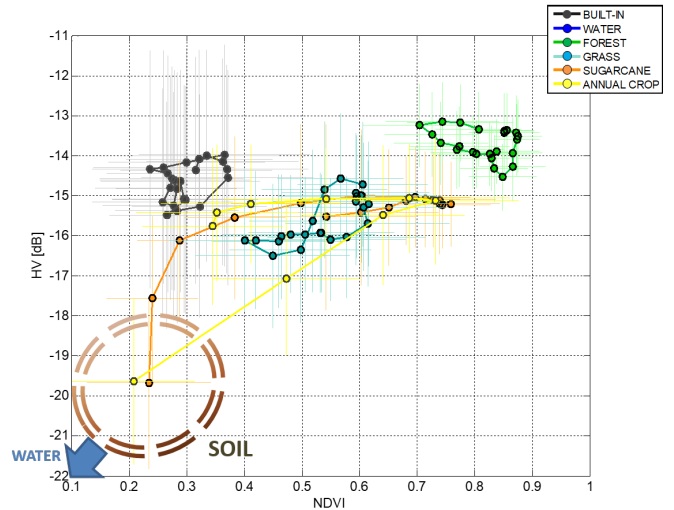


**Fig. 3.** Synoptic representation of the class signatures ( $\mathbf{m}$  - points,  $\mathbf{C}$ - errorbars) in the  $NDVI - HV$  [dB] space for the Sao Paulo area. Each point correspond to a different state for sugarcane and annual crops, whereas it corresponds to a different time for the other classes.

in order to determine the most likely scenario.

The probability of high or low water content in the scene at a specific date can be further derived by summation of the complementary pairs  $WW, DW$  or  $DD, WD$ . Uniform agreements on the most likely scenario over a relatively large number of fields provides a strong indication of a precipitation event or of a drought. Viceversa, strong discrepancies between fields can be a good indication of irrigation activities. Although the method has been presented as a standalone solution, mainly devoted to the detection of watering events, its intrinsic soft-labelling nature would strongly value an integration with other coarse-scale soil moisture products. The integration would have a two-fold benefit: 1) it would provide physical interpretation and calibration to the extracted  $\omega$  probabilities. 2) It would mitigate eventual errors occurring during the start of growth and the harvesting period due to large vegetation, and hence backscatter, dynamics.

#### 4. REFERENCES

- [1] S. C. Steele-Dunne, H. McNairn, A. Monsivais-Huertero, J. Judge, P. W. Liu, and K. Papathanassiou, "Radar remote sensing of agricultural canopies: A review," *IEEE Journal of Selected Topics in Applied Earth Observations and Remote Sensing*, vol. 10, no. 5, pp. 2249–2273, May 2017.
- [2] Y. Oh, K. Sarabandi, and F. T. Ulaby, "An empirical model and an inversion technique for radar scattering

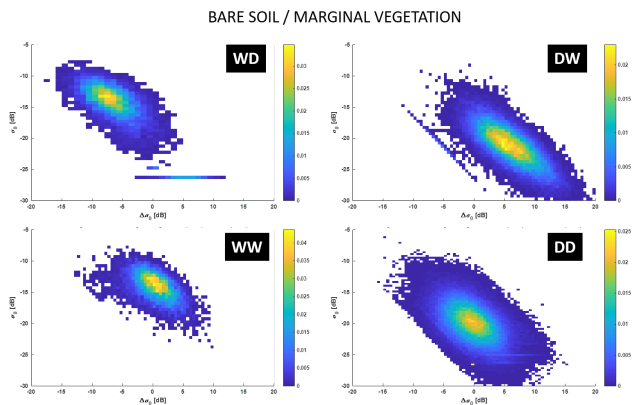


**Fig. 4.** Bare soil radar backscatter analysis. The bivariate distribution ( $HV$  [dB] -  $\Delta HV$  [dB]) associated to the 4 different water scenarios are reported: WD - Wet to Dry, DD - Dry to Dry, WW - Wet to Wet, DW - Dry to Wet.

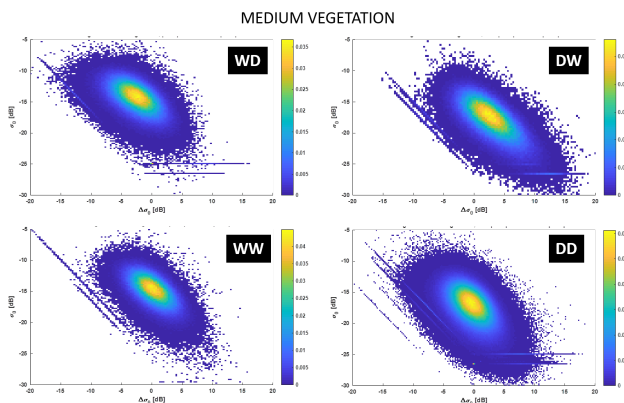


**Fig. 5.** Medium vegetation radar backscatter analysis. The bivariate distribution ( $HV$  [dB] -  $\Delta HV$  [dB]) associated to the 4 different water scenarios are reported.

from bare soil surfaces,” *IEEE Transactions on Geoscience and Remote Sensing*, vol. 30, no. 2, pp. 370–381, Mar 1992.

- [3] E. P. W. Attema and Fawwaz T. Ulaby, “Vegetation modeled as a water cloud,” *Radio Science*, vol. 13, no. 2, pp. 357–364, 1978.
- [4] S. Park, S. K. Kweon, and Y. Oh, “Validity regions of soil moisture retrieval on the LAI -  $\theta$  plane for agricultural fields at l-, c-, and x-bands,” *IEEE Geoscience and Remote Sensing Letters*, vol. 12, no. 6, pp. 1195–1198, June 2015.
- [5] Q. Liu, M. Zribi, M. J. Escorihuela, and N. Baghdadi, “Synergetic use of sentinel-1 and sentinel-2 data for soil moisture mapping at 100 m resolution,” *Sensors (Basel, Switzerland)*, vol. 17, no. 9, 2017.
- [6] J. Peng, A. Loew, O. Merlin, and N. E. C. Verhoest, “A review of spatial downscaling of satellite remotely sensed soil moisture,” *Reviews of Geophysics*, vol. 55, no. 2, pp. 341–366, 2017, 2016RG000543.
- [7] H. Lievens, R. H. Reichle, Q. Liu, G. J. M. De Lannoy, R. S. Dunbar, S. B. Kim, N. N. Das, M. Cosh, J. P. Walker, and W. Wagner, “Joint sentinel-1 and smap data assimilation to improve soil moisture estimates,” *Geophysical Research Letters*, vol. 44, no. 12, pp. 6145–6153, 2017, 2017GL073904.
- [8] O. A. Eweys, M. J. Escorihuela, J. M. Villar, S. Er-Raki, A. Amazirh, L. Olivera, L. Jarlan, S. Khabba, and O. Merlin, “Disaggregation of smos soil moisture to 100 m resolution using modis optical/thermal and sentinel-1 radar data: Evaluation over a bare soil site in morocco,” *Remote Sensing*, vol. 9, no. 11, 2017.
- [9] L. Brocca, T. Moramarco, F. Melone, and W. Wagner, “A new method for rainfall estimation through soil moisture observations,” *Geophysical Research Letters*, vol. 40, no. 5, pp. 853–858, 2013.
- [10] R. D. Koster, L. Brocca, W. T. Crow, M. S. Burgin, and G. J. M. De Lannoy, “Precipitation estimation using l-band and c-band soil moisture retrievals,” *Water Resources Research*, vol. 52, no. 9, pp. 7213–7225, 2016.
- [11] L. Iannini, R. Molijn, A. Mousivand, R. Hanssen, and R. Lamparelli, “A hmm-based approach for historic and up-to-date land cover mapping through landsat time-series in the state of sao paulo, brazil,” in *2016 IEEE International Geoscience and Remote Sensing Symposium (IGARSS)*, July 2016, pp. 5457–5460.